THE JOURNAL OF PHYSICAL CHEMISTRY A

Article

pubs.acs.org/JPCA

gem-Diol and Hemiacetal Forms in Formylpyridine and Vitamin-B_6-Related Compounds: Solid-State NMR and Single-Crystal X-ray Diffraction Studies

Ayelén Florencia Crespi,[†] Daniel Vega,[‡,#] Ana Karina Chattah,[⊥] Gustavo Alberto Monti,[⊥] Graciela Yolanda Buldain,[†,∥] and Juan Manuel Lázaro-Martínez*[,†,§]

[†]Departamento de Química Orgánica, Facultad de Farmacia y Bioquímica, Universidad de Buenos Aires, Junín 956 (C1113AAD), CABA, Argentina

[‡]Departamento de Física de la Materia Condensada, Comisión Nacional de Energía Atómica, Av. Gral. Paz 1499 (1650)San Martín, Buenos Aires, Argentina

[#]Escuela de Ciencia y Tecnología, Universidad Nacional de General San Martín, Buenos Aires, Argentina

[∥]CONICET, Godoy Cruz 2290 (C1425FQB), CABA, Argentina

[⊥]FaMAF-Universidad Nacional de Córdoba & IFEG-CONICET, Medina Allende s/n (X5000HUA), Córdoba, Argentina

[§]IQUIFIB-CONICET, Junín 956 (C1113AAD), CABA, Argentina

Supporting Information

ABSTRACT: The *gem*-diol moieties of organic compounds are rarely isolated or even studied in the solid state. Here, liquid- and solid-state NMR, together with single-crystal X-ray diffraction studies, were used to show different strategies to favor the *gem*-diol or carbonyl moieties and to isolate hemiacetal structures in formylpyridine and vitamin-B_6-related compounds. The change in position of the carbonyl group in pyridine compounds had a clear and direct effect on the hydration, which was enhanced by trifluoroacetic acid addition. Because of their biochemical importance, vitamin-B_6-related compounds were studied with emphasis on the elucidation of the *gem*-diol, cyclic hemiacetal or carbonyl structures that can be obtained in different experimental conditions. In particular, new racemic mixtures for the cyclic hemiacetal structure from pyridoxal are reported in trifluoroacetate and hydrochloride derivatives.

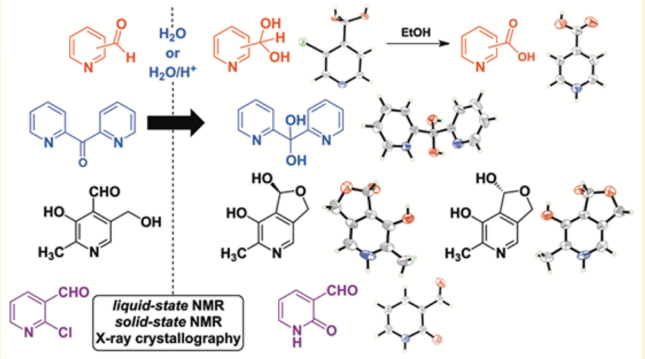

1. INTRODUCTION

The synthesis of novel molecules that act as ligands for various heavy metal ions, such as those containing *gem*-diol moieties in their structures, is a field that is being widely studied to obtain new polymeric materials and/or metal complexes due to the applications in the synthesis of paramagnetic 3d transition metal clusters.[1] A geminal diol or *gem*-diol is the product of the addition of water to a carbonyl group of an aldehyde or ketone. Such compounds are rarely stable and infrequently observed in the liquid or solid state since the moisture balance is largely dependent on the structure. For example, 99.99% of formaldehyde but only 58% of acetaldehyde in water at 20 °C exist in the hydrated form.[2] In turn, these structures are rare and can seldom be isolated as such, because they quickly revert to the aldehyde or ketone that originated them. However, we have previously reported the isolation of a *gem*-diol form for the 2-imidazolecarboxaldehyde molecule, with no remainder of the aldehyde moiety in the solid state.[3]

In particular, imidazole and pyridine molecules containing carbonyl groups are widely used for the synthesis of metal complexes with relevance in medicinal and coordination chemistry.[4−6] Sartzi et al. studied the use of di(2-pyridyl) ketone [$(Py)_2C{=}O$] as an organic ligand for the synthesis of metal complexes.[7] Efthymiou et al. expanded the number and variety of carbonyl compounds but observed the *gem*-diol form only when the X-ray crystallographic analysis was done in single-crystal samples corresponding to metal complexes formed from carbonyl ligands.[8] Tasiopoulos and Perlepes studied formylpyridine compounds for the development of coordination complexes with transition metal ions, with an emphasis on "diolate high-spin molecules" and "single-molecule magnets".[1,9] In particular, the synthesis of new single-molecule magnets is of great interest because they are promising

Received: August 4, 2016
Revised: September 13, 2016
Published: September 15, 2016

DOI: 10.1021/acs.jpca.6b07898
J. Phys. Chem. A 2016, 120, 7778−7785

candidates to be applied in spintronics and quantum computing.[10−13]

gem-Diol moieties in metal complexes containing pyridine carbonyl compounds have so far been elucidated through single-crystal X-ray diffraction studies, but the electronic effects of the ligands have been not taken into account. In this sense, a Cu(II) complex with 2-formylpyridine molecules (**A**$_1$) presents the *gem*-diol moiety in single crystals obtained from water solutions and $CuCl_2$,[14] demonstrating that the presence of water affects the functionalization of the ligand, preventing the aldehyde form in the crystal lattice of the copper complex. In contrast, the lower reactivity of the aldehyde group in 3-formylpyridine (**A**$_3$) toward the addition of water explains that, in the different reported complexes with copper[15] or zinc[16] ions, the formyl group remains in aqueous media. Furthermore, the aldehyde moiety has been observed for zinc complexes of 2-formylpyridine (**A**$_1$) when the single crystals were obtained from dissolutions in CH_2Cl_2 or CH_2Cl_2/THF with addition of petroleum ether (bp 70−90 °C) in the absence of water molecules.[17] Moreover, a rhenium complex with **A**$_1$ in methanol renders the hemiacetal structure[18] as a consequence of the addition of methanol to the aldehyde group in **A**$_1$, due to the higher reactivity of the formyl moiety at the second position of the pyridine system than at the third one in 3-formylpyridine compound (**A**$_2$). However, no reports of metal complexes containing the 4-formylpyridine molecules (**A**$_3$) have yet been reported. In addition, no nuclear magnetic resonance (NMR) studies have been performed to these compounds. In particular, solid-state NMR (*ss*-NMR) has allowed overcoming the challenges inherent in studying noncrystalline materials that cannot be characterized by single-crystal X-ray diffraction techniques, being an ideal technique to focus on the possibility to render the *gem*-diol forms and their stability, obtained from the corresponding carbonyl monomers commonly used in the area.[1,14,17−23]

In this context, the aim of this work was to study the *gem*-diol generation in pyridine molecules bearing carbonyl groups. In addition, vitamin-B_6-related compounds were analyzed due to their importance in biochemical processes,[24,25] with emphasis on the structural elucidation that can be observed in their reactions.[26−28] Liquid-state (*ls*-NMR) and *ss*-NMR and single-crystal X-ray diffraction techniques were used to elucidate the *gem*-diol or carbonyl moieties and the possibility to isolate hemiacetal structures in some cases.

2. EXPERIMENTAL SECTION

2.1. Synthesis. Trifluoroacetic acid (TFA, 99%), 2-formylpyridine (**A**$_1$, 99%), 3-formylpyridine (**A**$_2$, 98%), 4-formylpyridine (**A**$_3$, 97%), 3-chloro-4-formylpyridine (**A**$_4$, 97%), 2-chloro-3-formylpyridine (**A**$_5$, 97%), di(2-pyridyl) ketone (**K**$_6$, 99%), pyridoxal hydrochloride (**A**$_7$**·HCl**, ≥ 99%), pyridoxal-5′-phosphate (**A**$_8$, ≥ 98%), deuterium oxide (D_2O, 99.9 atom %D) and dimethyl sulfoxide-d_6 (DMSO-d_6, 99.96 atom %D) were purchased from Sigma-Aldrich and were used without further purification.

The general quantitative synthesis of the corresponding neutral *gem*-diol solid forms for 4-formylpyridine (**A**$_3$) and 3-chloro-4-formylpyridine (**A**$_4$) consists in dissolving 40 mmol of **A**$_3$ or **A**$_4$ in 3 mL of distilled water, which produces the spontaneous crystallization of the *gem*-diol compounds (**H**$_{3\ \text{melting point}}$ = 70−72 °C and **H**$_{4\ \text{melting point}}$ = 84−86 °C).

The solid pyridinium-trifluoroacetate derivatives containing *gem*-diol (**H**$_1$**·TFA and H**$_3$**·TFA**) or carbonyl moieties (**A**$_2$**·TFA**), were obtained by incubation of 50 mmol of **A**$_1$, **A**$_2$, and **A**$_3$ in 3 mL of a solution of 1% of water in TFA for 24 h at room temperature. Then, the TFA solutions were lyophilized and the solid samples were collected and stored in a desiccator prior to the NMR measurements. In particular, when the trifluoroacetate derivatives from **A**$_{2-3}$ (50 mmol) were placed in 5 mL of ethanol 95% for 72 h at room temperature and then dried under vacuum, they were completely oxidized to the corresponding carboxylic acid compounds (**CA**$_{2-3}$**·TFA**).

The solid hydrochloride pyridoxal (**A**$_7$**·HCl**) was obtained by incubation of pyridoxal (50 mmol) in 20 mL of HCl 5% for 72 h at room temperature, respectively. Then, the sample was lyophilized and the solid sample was collected and stored in a desiccator prior to the NMR measurements. The solid trifluoroacetate derivative **A**$_7$**·TFA** was obtained by incubation of **A**$_7$**·HCl** (50 mmol) in 10 mL of TFA 30% for 72 h at room temperature. Then, the sample was treated as in **A**$_7$**·HCl**.

2.2. NMR Experiments. High-resolution ^{13}C solid-state spectra for the different compounds were recorded using the ramp $^1H-^{13}C$ CP-MAS sequence (cross-polarization and magic angle spinning) with proton decoupling during acquisition. All the *ss*-NMR experiments were performed at room temperature in a Bruker Avance-II 300 spectrometer equipped with a 4 mm MAS probe. The operating frequency for protons and carbons was 300.13 and 75.46 MHz, respectively. Glycine was used as an external reference for the ^{13}C spectra and to set the Hartmann−Hahn matching condition in the cross-polarization experiments in ^{13}C spectra. The recycling time was set at 4 s, to obtain a compromise between the signal-to-noise ratio in a single scan and the total time of the experiments performed with a number of scans between 2000 and 4000.

The contact time during CP was 1500 μs for ^{13}C spectra for all the samples. The SPINAL64 sequence (small phase incremental alternation with 64 steps) was used for heteronuclear decoupling during acquisition with a proton field H_{1H} satisfying $\omega_{1H}/2\pi = \gamma_H H_{1H}$ = 62 kHz.[29] The spinning rate for all the samples was 10 kHz.

The *ls*-NMR experiments were performed at room temperature in a Bruker Avance-II 300, 500 or Ascend-600 spectrometer. To determine the hydration of the carbonyl group, ∼30 mg of each compound was dissolved in a D_2O or D_2O solution containing 1% of TFA.

2.3. Single-Crystal X-ray Studies. Single-crystal samples were isolated from the slow evaporation of each solution at room temperature where the compound of interest was dissolved or obtained as mentioned above.

Single-crystal X-ray diffraction data were collected at room temperature, using a Gemini A diffractometer, Oxford Diffraction, Eos CCD detector with graphite-monochromated Mo Kα (λ = 0.71073 Å) radiation. Data-collection strategy and data reduction followed standard procedures implemented in the CrystAlisPro software. Different independent reflections were collected for each sample and they are specified in the Supporting Information. The structures were solved using SHELXS-97 program[30] and refined using the full-matrix LS procedure with SHELXL-2014/7.[31] Anisotropic displacement parameters were employed for non-hydrogen atoms. All hydrogen atoms were located at the expected positions and they were refined using a riding model.

3. RESULTS AND DISCUSSION

3.1. Studies in Formylpyridines. In order to study the reactivity of water addition in formylpyridine isomers, each

DOI: 10.1021/acs.jpca.6b07898
J. Phys. Chem. A 2016, 120, 7778−7785

Table 1. Amount of *gem*-Diol and Aldehyde Forms for the Indicated Carbonyl Compounds Determined by ^{1}H NMR

	^{1}H NMR experiment			
	D_2O		D_2O-TFA	
compound	*gem*-diol	aldehyde	*gem*-diol	aldehyde
2-CHO-pyridine ($\mathbf{A_1}$)	40	60	100	–
3-CHO-pyridine ($\mathbf{A_2}$)	10	90	85	15
4-CHO-pyridine ($\mathbf{A_3}$)	50	50	100	–
3-Cl-4-CHO-pyridine ($\mathbf{A_4}$)	83 (47)[a]	17 (53)[a]	100	–
2-Cl-3-CHO-pyridine ($\mathbf{A_5}$)[b]	41 (–)[a]	59 (100)[a]	60	40
di(2-pyridyl) ketone ($\mathbf{K_6}$)	3	97[c]	100	–
pyridoxal·HCl ($\mathbf{A_7}$·**HCl**)	100[d]	–	100[d]	–
pyridoxal-5′-phosphate ($\mathbf{A_8}$)[e]	73.8 (94)[a]	26.2 (6)[a]	75.2[b]	24.8[b]

[a]In DMSO-d_6. [b]The reported values are related to the relative content of the *gem*-diol and aldehyde forms since other compounds are also present in the mixture (see the text and Supporting Information for additional details). [c]The reported value is for the ketone form. [d]The reported values refer to the cyclic hemiacetal in D_2O, D_2O-TFA and DMSO-d_6. However, the *gem*-diol moiety was quantitatively obtained when the solid $\mathbf{A_7}$·**HCl** was treated with D_2O/NaOH solution. [e]The aldehyde form was quantitatively obtained when the solid $\mathbf{A_8}$ was treated with D_2O/NaOH.

compound was dissolved in D_2O and studied by *ls*-NMR experiments (Table 1). The ^{1}H NMR spectra for all the isomers showed the presence of the *gem*-diol moieties in D_2O at a proton chemical shift around (-C**H**$(OH)_2$) depending on the position in the pyridine ring (Figure 1 and Supporting Information). On the basis of the integration of each ^{1}H NMR signal for the *gem*-diol ($\delta(^1H)$ = 5.70–6.30 ppm) and/or the aldehyde ($\delta(^1H)$ = 9.19–10.40 ppm), it was possible to obtain the relative content in terms of each functional moiety (Table 1). From these results, we concluded that the most reactive compound for the addition of water was 4-formylpyridine ($\mathbf{A_3}$) (54%) followed by 2-formylpyridine ($\mathbf{A_1}$) (44%) and 3-formylpyridine ($\mathbf{A_2}$) (11%). This fact is justified given the π-deficient character of the pyridine ring where the most electron-deficient positions are 2, 4, and 6 in comparison with 3 and 5, explaining that 3-formylpyridine had the lowest hydrate percent. Moreover, the complete hydration in 2- and 4-formylpyridines can be obtained with 1% of TFA in D_2O according with the ^{1}H NMR spectrum (Figure 1). However, $\mathbf{A_2}$ was not completely hydrated even with a higher TFA concentration (Table 1) since the third position of the pyridine system was not equally affected by the inductive effect of the system in comparison with the other positions.

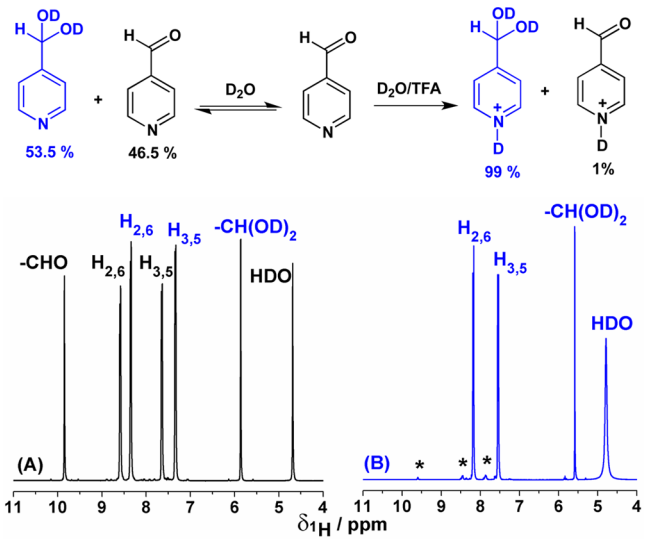

Figure 1. ^{1}H NMR spectra for 4-formylpyridine ($\mathbf{A_3}$) in the presence of D_2O (A) and D_2O–TFA (B). The asterisk in spectrum B indicates the residual signal of the carbonyl form.

Since all the formylpyridine isomers are liquid at room temperature, we prepared the solid trifluoroacetate derivatives to be studied by *ss*-NMR, and, in the cases where the substance rendered single crystals, they were studied through X-ray diffraction. Figure 2 shows the ^{13}C CP-MAS spectra for the products obtained for the corresponding trifluoroacetate derivatives or neutral form of the formylpyridines and other related solid compounds commercially available.

Even when all the pyridine derivatives were incubated in TFA under the same experimental conditions, depending on the position of the formyl group, it was possible to isolate solids where the aldehyde or *gem*-diol content was different. The ^{13}C CP-MAS spectra (Figure 2A and Figure 2B) showed that, in TFA, $\mathbf{A_1}$ presented the *gem*-diol moieties ($\delta(^{13}C)$ = 73.3 ppm, –**C**H$(OH)_2$, Figure 2A), whereas $\mathbf{A_2}$ crystallized as the corresponding aldehyde ($\mathbf{A_2}$·**TFA**) ($\delta(^{13}C)$ = 188.2 ppm, –**C**HO, Figure 2B). In contrast, when $\mathbf{A_2}$·**TFA** was incubated in ethanol, single crystals of 3-carboxypyridine ($\mathbf{CA_2}$·**TFA**) were obtained ($\delta(^{13}C)$ = 166.3 ppm, –**C**O_2H, Figure 2C). However, this crystallographic structure has been previously reported.[32] The ^{13}C CP-MAS spectrum for $\mathbf{CA_2}$·**TFA** showed that the oxidation of the formyl group in $\mathbf{A_2}$ was completed in this condition since no signals of the aldehyde form ($\mathbf{A_2}$) were observed in the *ls*- or *ss*-NMR spectra (Figure 2C). These results indicate that the solid-state NMR through ^{13}C CP-MAS spectra is the best screening for the identification of the *gem*-diol groups in a solid sample by observing the range of 70–100 ppm of ^{13}C chemical shift. This must be done prior to the dissolution in deuterated solvents where the proportion of carbonyl and *gem*-diol moieties change depending on the properties of the medium, not being representative of the real content in the solid state. In addition, a salt was formed between the pyridine compounds and TFA, which was evidenced from the signal of the carboxylate group at 160.5 ppm ($CF_3CO_2^-$) and the carbon corresponding to the trifluoromethyl group ($CF_3CO_2^-$) at ~120 ppm in the ^{13}C CP-MAS spectra.[33]

Interestingly, in a particular ratio of 4-formylpyridine:water (4 mL:3 mL), it was possible to obtain single crystals suitable for X-ray studies and to find the corresponding *gem*-diol form in the solid state. However, González-Mantero et al. have previously reported the corresponding structure as a byproduct of a particular chemical reaction where the *gem*-diol form was

DOI: 10.1021/acs.jpca.6b07898
J. Phys. Chem. A 2016, 120, 7778–7785

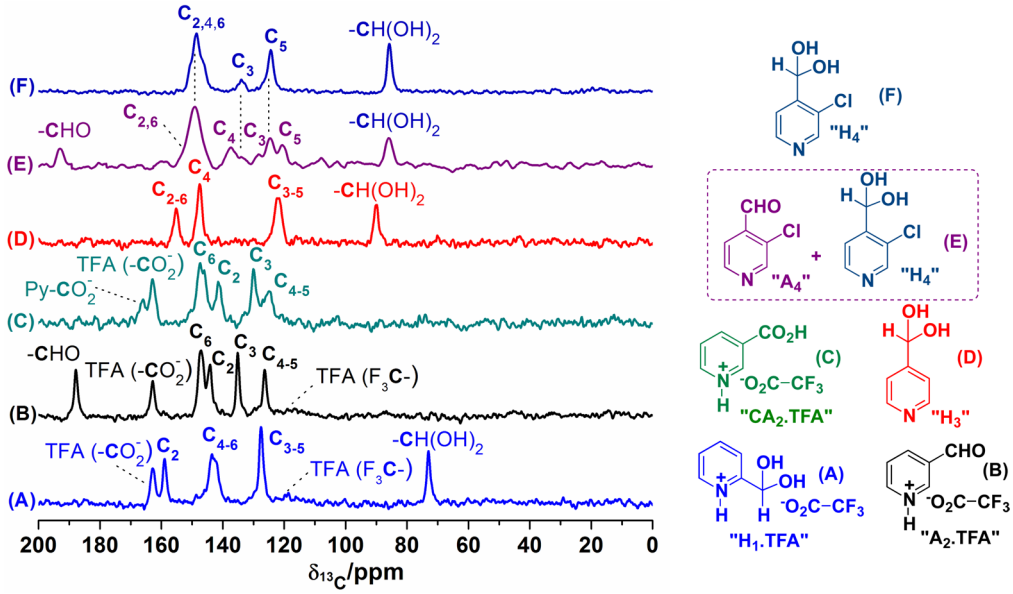

Figure 2. ^{13}C CP-MAS spectra for the solids obtained after the treatment of the following compounds in different experimental conditions: 2-formylpyridine ($\mathbf{A_1}$) in TFA ($\mathbf{H_1}$·**TFA**, A), 3-formylpyridine ($\mathbf{A_2}$) in TFA ($\mathbf{A_2}$·**TFA**, B), the $\mathbf{A_2}$·**TFA** treated with ethanol ($\mathbf{CA_2}$·**TFA**, C), the solid obtained with 4-formylpyridine ($\mathbf{A_3}$) in water ($\mathbf{H_3}$, D), the solid commercial sample of 3-chloro-4-formylpyridine ($\mathbf{A_4}$) ($\mathbf{A_4}$ + $\mathbf{H_4}$, E), and the solid obtained after the treatment of $\mathbf{A_4}$ with water ($\mathbf{H_4}$, F).

not the objective of the work.[34] Also, Majerz et al. studied a ionic adduct between $\mathbf{A_3}$ and 2,6-dichloro-4-nitrophenol.[35] In the same way, 4-formylpyridine ($\mathbf{A_3}$) rendered quantitative solid sample under the *gem*-diol form ($\mathbf{H_3}$) from the treatment of $\mathbf{A_3}$ with water (5 mL:3 mL), although the 4-carboxypyririne ($\mathbf{CA_3}$) was elucidated by X-ray results obtained from the incubation of the trifluoroacetate sample of $\mathbf{H_3}$ in ethanol (Figure 3). On the other hand, the solid aldehyde 3-chloro-4-

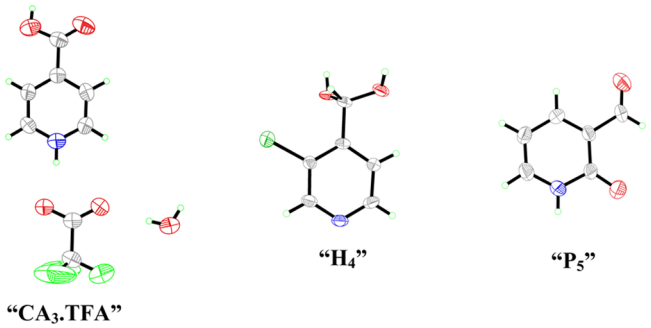

Figure 3. Crystal structures for 4-carboxypyridineium trifluoroacetate ($\mathbf{CA_3}$·**TFA**), *gem*-diol form of 3-chloro-3-formylpyridine ($\mathbf{H_4}$), and 3-formyl-2-pyridone ($\mathbf{P_5}$). The displacement ellipsoids for the non-H atoms in the figure were drawn at the 50% probability level.

formylpyridine ($\mathbf{A_4}$) commercially available is in a mixture of aldehyde:*gem*-diol of 0.53:0.47 according with the ^{1}H NMR spectrum in DMSO-d_6. When the solid $\mathbf{A_4}$ was treated with water, the *gem*-diol crystallized as the only product according with the *ss*-NMR spectrum (Figure 2F and Table 1). Moreover, single crystals for $\mathbf{H_4}$ were analyzed by X-ray diffraction, showing the *gem*-diol moieties in the crystal lattice (Figure 3 and Figure S27 and Figure S28).

For the 2-chloro-3-formylpyridine ($\mathbf{A_5}$), only the aldehyde form (92.6%) was present and a minority content of the 3-formyl-2-pyridone ($\mathbf{P_5}$, 7.4%) was observed in the ^{1}H NMR spectrum in DMSO-d_6 (Figure S13). When these solid chloroformylpyridines ($\mathbf{A_{4-5}}$) were dissolved in D_2O, the *gem*-diol content increased in each sample in comparison with the results in DMSO-d_6 according to NMR results. This is indicative of the higher reactivity of the nucleophilic addition of water to the aldehyde group than the corresponding derivatives without chlorine in their structure (Table 1). Interestingly, the ^{1}H NMR spectrum of 2-chloro-3-formyl-pyridine ($\mathbf{A_5}$) in D_2O showed that the contents of aldehyde and *gem*-diol forms were 21.3 and 14.7%, respectively. The remaining 64% was associated with a 3-formyl-2-pyridone ($\mathbf{P_5}$) as a consequence of the nucleophilic substitution of chlorine by water molecules (Figure S11). It is important to point out that the incubation of $\mathbf{A_5}$ in water rendered single crystals, where the 2-pyridone structures were elucidated by X-ray diffraction studies (Figure 3, Figure S29 and Figure S30). These results indicate that the fact that 3-formyl-2-pyridone ($\mathbf{P_5}$) was obtained in 64% in water was due to the higher reactivity for the nucleophilic aromatic substitution than the addition of water to the carbonyl group at the third position of the aromatic system in $\mathbf{A_5}$. Thus, the *gem*-diol form ($\mathbf{H_5}$) was obtained in 14.7% with 21.3% of the aldehyde ($\mathbf{A_5}$) (Table 1). The same analysis in D_2O–TFA showed that the amounts of aldehyde, *gem*-diol, and 2-pyridone forms for $\mathbf{A_5}$ were 38.6%, 57.9%, and 3.5%, respectively, indicative that the acidic medium increases the addition of water to the aldehyde group against the substitution of the chloride at the second position (Table 1).

Finally, a di(2-pyridyl) ketone ($\mathbf{K_6}$) was studied in the liquid-state in D_2O, where only 3% was hydrated, giving rise to the *gem*-diol moiety in the ^{1}H NMR spectrum (Table 1). Also, the treatment of $\mathbf{K_6}$ with water rendered a solid where, according with the ^{13}C CP-MAS spectrum (Figure 4A), only the ketone form was present. Even when the ketone carbon is next to the second position of both electron-withdrawing pyridine rings, the effect on the nucleophilic addition of water cannot be observed in D_2O solution since only 3% corresponded to the

DOI: 10.1021/acs.jpca.6b07898
J. Phys. Chem. A 2016, 120, 7778−7785

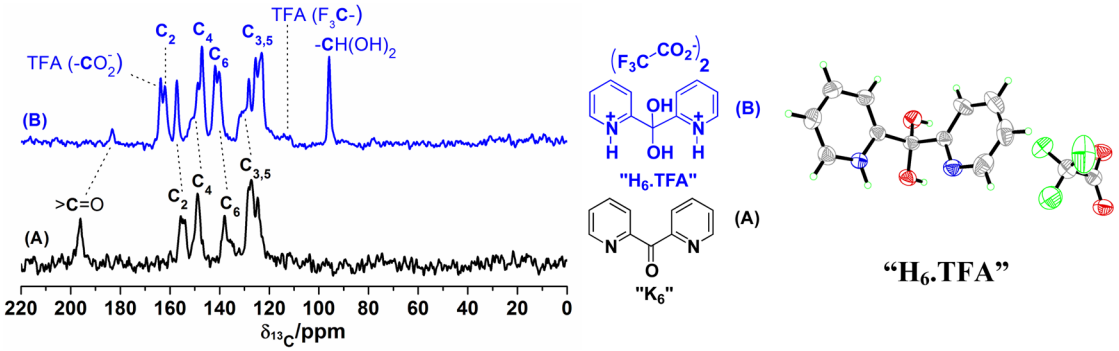

Figure 4. ^{13}C CP-MAS spectra for the commercial solid of the di(2-pyridyl) ketone ($\mathbf{K_6}$) (A) and $\mathbf{K_6}$ treated with TFA ($\mathbf{H_6{\cdot}TFA}$ + $\mathbf{K_6{\cdot}TFA}$) (B). Crystal structure for $\mathbf{H_6{\cdot}TFA}$. The displacement ellipsoids for the non-H atoms in the figure were drawn at the 50% probability level.

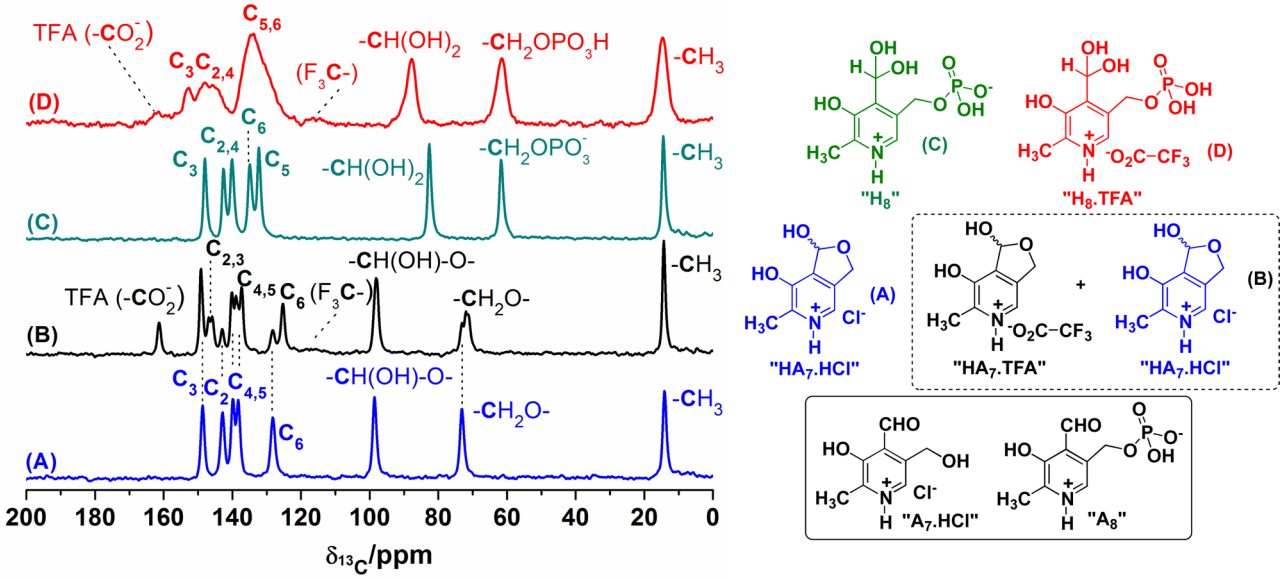

Figure 5. ^{13}C CP-MAS spectra for pyridoxal·HCl ($\mathbf{HA_7{\cdot}HCl}$, A), pyridoxal·HCl incubated with TFA ($\mathbf{HA_7{\cdot}HCl}$ + $\mathbf{HA_7{\cdot}TFA}$, B), pyridoxal-5′-phosphate ($\mathbf{H_8}$, C), and pyridoxal-5′- phosphate treated with TFA ($\mathbf{H_8{\cdot}TFA}$, D).

gem-diol form, and it was necessary to add TFA to force the reaction (Table 1). A possible explanation may be the hydrophobic:hydrophilic balance of the molecule, which disfavors the nucleophilic attack of water. Then, the addition of TFA to an aqueous solution containing $\mathbf{K_6}$ produced the *gem*-diol form in an excellent yield as well as single crystals, demonstrating again the *gem*-diol moiety and the disposition of the aromatic rings in the crystal lattice (Figure 4). The ^{13}C CP-MAS spectrum for the TFA crystals obtained from $\mathbf{K_6}$ ($\mathbf{H_6{\cdot}TFA}$ + $\mathbf{K_6{\cdot}TFA}$) shows that most of the compound is present as *gem*-diol form with traces of the ketone moieties, having into account the ^{13}C resonance signal at 183.3 ppm, which presents a shift to low frequency values after the protonation of the pyridine system in comparison with the nonprotonated di(2-pyridyl) ketone (δ(^{13}C): 196.4 ppm, >C═O, Figure 4). The TFA crystals of $\mathbf{K_6}$ ($\mathbf{H_6{\cdot}TFA}$ + $\mathbf{K_6{\cdot}TFA}$) dissolved in D_2O showed a similar amount of both *gem*-diol and ketone forms. However, the NMR spectrum in DMSO-d_6 shows only the ketone form (Figure S24), being not representative of the solid composition according with the *ss*-NMR. The X-ray results demonstrated the *gem*-diol structure for $\mathbf{K_6}$ ($\mathbf{H_6{\cdot}TFA}$, Figure 4). The hydrated structure was first reported for a hydrochloride form of $\mathbf{H_6}$ with structural differences in the crystal lattice since both nitrogens of the pyridine rings were in opposite direction.[36] In contrast, in the TFA salt reported here, both nitrogens are in the same side and the *gem*-diol is linked by hydrogen bonds with the carboxyl group of TFA (Figure 4 and Supporting Information). Regarding reported metal complexes, the *gem*-diol forms were observed in Cu(II) or Ni(II) centers synthesized from $\mathbf{K_6}$ where the *gem*-diol structure is stabilized by coordination with less importance of the metal ion and the anion used in their preparation.[37,38] The hydration of the carbonyl group is enhanced by the slight acidification of the medium since in aqueous solution only 3% of the *gem*-diol is present, in agreement with our results reported here (Table 1).

3.2. Vitamin-B_6-Related Compounds. Pyridoxal ($\mathbf{A_7}$) and pyridoxal-5′-phosphate ($\mathbf{A_8}$) compounds were studied having into account their biochemical importance due to their role as coenzymes in different enzymatic reactions (Figure 5). The ^{13}C CP-MAS spectrum for a hydrochloride pyridoxal ($\mathbf{A_7{\cdot}HCl}$) sample was performed and the results are shown in Figure 5A. The *ss*-NMR spectrum indicated the absence of the aldehyde around 180−200 ppm and the presence of the corresponding *gem*-diol or hemiacetal moieties at 98.7 ppm. However, the *ls*-NMR clearly showed that the cyclic hemiacetal form ($\mathbf{HA_7{\cdot}HCl}$) was present for this molecule due to the magnetic inequivalence of the protons of the methylene group.[39] The

DOI: 10.1021/acs.jpca.6b07898
J. Phys. Chem. A 2016, 120, 7778−7785

two doublets present at 5.32 and 5.14 ppm with a J_{gem} coupling of 13.8 Hz in the ^{1}H NMR spectrum demonstrate the cyclization involving the hydroxymethylene and the carbonyl group (Figure 5 and Figure S14).

The single-crystal X-ray diffraction structure resolved for the TFA salts allowed us to confirm the cyclic hemiacetal formation together with the racemic structure that can also be discriminated (Figure 6), something that is not possible from the NMR spectra in Figure 5. Manohar et al. reported the X-ray structure for the pyridoxal molecule in the neutral form, where the hemiacetal and the zwitterionic forms were present, but the racemic mixture was not obtained.[40] Our results show that the racemization takes place due to the intramolecular cyclization and is equally probable for both sides of the planar formyl group, rendering a racemic sample that was evidenced with the X-ray results (Figure 6). Since the racemization cannot be deduced from the NMR spectra, optical rotation experiments were performed. The aqueous solutions of the crystalline pyridoxal·TFA (**HA$_7$·TFA**) or pyridoxal·HCl (**HA$_7$·HCl**) samples were optically inactive, meaning that there is no net rotation of the plane-polarized light due to the racemic mixture in both solids.

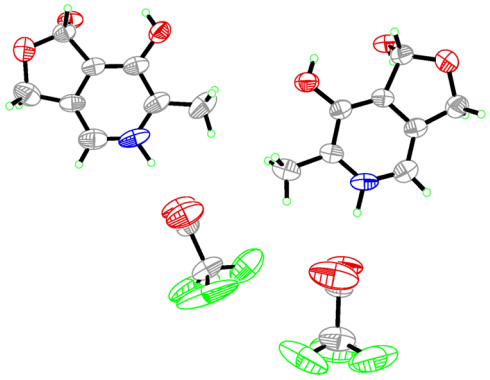

Figure 6. Crystal structure for pyridoxal·TFA racemate (**HA$_7$·TFA**). The displacement ellipsoids for the non-H atoms in the figure were drawn at the 50% probability level.

Furthermore, even when the single-crystal structure was studied only for the pyridoxal·TFA compound, the ^{13}C CP-MAS for the TFA salt provided additional information concerning the composition of the crystalline powder obtained after the treatment with TFA of an aqueous solution of the hydrochloride pyridoxal. Spectrum B in Figure 5 shows the presence of both chloride and trifluoroacetate as contra-ion of the cationic pyridinium system from the pyridoxal molecule, being possible the discrimination of both molecules due to the different environments of each pyridine system depending on its anion (Figure 5). The splitting of the NMR signals may indicate the presence of two molecules per unit cell in Figure 5B. However, as determined by X-ray fluorescence, the **HA$_7$·TFA** sample still contains a chlorine content of 3.30 ± 0.10%, indicative of hydrochloride content in the **HA$_7$·TFA** solid sample. Also, some of the chemical shifts are observed for **HA$_7$·HCl** in the **HA$_7$·TFA** solid sample in comparison with the pure **HA$_7$·HCl** sample.

The *ls*-NMR results for the pyridoxal hydrochloride in both D_2O and D_2O−TFA showed that only the cyclic hemiacetal structure is present and stable. However, when the ^{1}H spectrum was recorded in D_2O−NaOH, the corresponding *gem*-diol form was observed, taking into account that the protons of the methylene group resonate as a singlet at 4.50 ppm, indicating that the hemiacetal structure has been affected by the alkaline medium. The *gem*-diol proton can be observed at 6.39 ppm (Figure S16). Although the single-crystal X-ray structure for the pyridoxal hydrochloride (**A$_7$·HCl**) has been previously reported by Fujiwara et al.,[41] where the aldehyde structure was present, our results presented here show that the cyclic hemiacetal structure for **A$_7$·HCl** and **A$_7$·TFA** is the only structure present according with the *ss*-, *ls*-NMR and X-ray results.

The last compound analyzed in this work was the pyridoxal-5′-phosphate (**A$_8$**), which presented a well-resolved ^{13}C CP-MAS spectrum (Figure 5C) for the *gem*-diol form (**H$_8$**), since in this molecule the formation of a cyclic hemiacetal as in pyridoxal is not possible due to the phosphate group at the hydroxylmethylene group at the fifth position of the pyridine ring. The single-crystal X-ray structure for **A$_8$** has been previously resolved by Fujiwara et al.[42] Nevertheless, the solid was analyzed by *ss*-NMR and the result is shown in Figure 5C. The *gem*-diol form was present for the pyridoxal-5′-phosphate in the commercial sample treated in water or TFA:water (1:0.01) solution. Also, a shift in the *gem*-diol carbon from 82.6 to 88.0 ppm can be observed with the formation of the TFA salt (Figure 5). The *ls*-NMR results in D_2O for a commercial sample of pyridoxal-5′-phosphate showed that the *gem*-diol and the aldehyde forms were present in 73.8% and 26.2%, respectively. However, the ^{13}C CP-MAS spectra only shows the *gem*-diol form (Figure 5). The ^{1}H NMR spectrum in D_2O-TFA shows a similar amount of *gem*-diol (75.2%) but a lower amount of aldehyde (21.6%), since some phosphate hydrolysis occurred with the concomitant formation of *gem*-diol and cyclic hemiacetal forms of the pyridoxal molecule in 3%, according with the NMR spectrum (Figure S20). Then, the pyridoxal-5′-phosphate was dissolved in DMSO-d_6 and the results were completely different, since the aldehyde and *gem*-diol contents were 94% and 6%, respectively. Once again, as in other compounds described in this work, DMSO-d_6 is not the best solvent to study the "real composition" of the samples in the solid state, but it is useful if the aldehyde form is desired in solution for any reason. In addition, the ^{1}H NMR results for the pyridoxal-5′-phosphate in D_2O-NaOH produced only the aldehyde form in 100% (Figure S21).

4. CONCLUSIONS

By using both *ls*- and *ss*-NMR, we studied the generation and stability of the *gem*-diol forms in various pyridine derivatives containing carbonyl groups. In general, *ss*-NMR was useful to determine the presence of *gem*-diols in the solid state in cases where the crystals obtained were not suitable for single-crystal X-ray diffraction studies or where the solvent in the *ls*-NMR altered the chemical structure of the molecule under study. However, in many cases, it was possible to analyze the data from both methods of structural characterization to complement and enhance the knowledge in the chemistry of *gem*-diol compounds.

The limitation of analytical techniques for the characterization of the *gem*-diol/carbonyl (aldehyde or ketone) content for a particular formyl or ketone compound is the balance obtained in a particular solvent. For that reason, throughout the manuscript, it is mentioned that for example the DMSO-d_6 solvent is not the best medium for the characterization at the liquid state, being the *ss*-NMR the best technique for the screening at the solid state, taking into account the inherent

DOI: 10.1021/acs.jpca.6b07898
J. Phys. Chem. A 2016, 120, 7778−7785

problem of low sensitivity. Common HPLC techniques can be used, but the problem is that the sample needs to be dissolved in acid/water mixtures, being easier to analyze only the NMR information from the solution state in the presence of H^+ species.

The hydration studies indicated that the position of the carbonyl group was essential to stabilize the *gem*-diol form, allowing their isolation and characterization in the solid state. The hydration process of formylpyridine compounds was favored due to the electron-withdrawing character of the aromatic system, with 2- and 4-formylpyridines being particularly stable. Also, the oxidation to carboxylic acid in some of the compounds studied here was obtained from the trifluoroacetate derivatives of formylpyridines according to the NMR and X-ray results.

The structural characterization by X-ray crystallography and *ss*-NMR techniques of vitamin-B_6-related compounds allowed identification of a cyclic hemiacetal form for the pyridoxal molecule, which was present with both TFA and HCl mediums. In addition, the racemization of the pyridoxal molecules demonstrated in acidic medium due to the intramolecular cyclization is equally probable for both sides of the planar formyl group, rendering a racemic sample that was evidenced with the X-ray results.

Indeed, the results presented here explain some structural characteristics observed in metal ion complexes where the *gem*-diol, carbonyl, or hemiacetal moieties are present, depending on the monomer used. This would allow a smart design of new metal complexes by using some of the compounds studied here and different metal ions, in a variety of experimental conditions. This will allow one to expand the chemistry in metal complexes and single-molecule magnets in terms of structural diversity of the ligands.

■ ASSOCIATED CONTENT

Supporting Information

The Supporting Information is available free of charge on the ACS Publications website at DOI: 10.1021/acs.jpca.6b07898.

Supplementary crystallographic information for each compound and *ls*-NMR spectra for all the compounds studied in the present work (PDF)

■ AUTHOR INFORMATION

Corresponding Author

*(J.M.L.-M.) Telephone/fax: +54-11-5287-4323. E-mail: lazarojm@ffyb.uba.ar and jmlazaromartinez@gmail.com.

Notes

The authors declare no competing financial interest.

Structural data of **CA_3·TFA** (CCDC No.1471042), **H_4** (CCDC No. 1471040), **P_5** (CCDC No. 1471035), **H_6·TFA** (CCDC No. 1471038), **HA_7·TFA** (CCDC No. 1471043) compounds were deposited as CIF files at the Cambridge Crystallographic Database and can be downloaded freely from the site: http://ccdc.cam.ac.uk.

■ ACKNOWLEDGMENTS

We express thanks for the financial support from ANPCYT (PICT 2012-0151), Universidad de Buenos Aires (UBACyT 2013-2016/043BA), CONICET (PIP 2014-2016/130), and SeCyT Universidad Nacional de Córdoba. We also thank María Victoria González-Eusevi for the English grammar corrections.

■ REFERENCES

(1) Tasiopoulos, A. J.; Perlepes, S. P. Diol-Type Ligands as Central "Players" in the Chemistry of High-Spin Molecules and Single-Molecule Magnets. *Dalton Trans.* **2008**, *41*, 5537−5555.

(2) March, J. *Advanced Organic Chemistry*; Wiley: New York, 1992.

(3) Lázaro Martínez, J. M.; Romasanta, P. N.; Chattah, A. K.; Buldain, G. Y. NMR Characterization of Hydrate and Aldehyde Forms of Imidazole-2-Carboxaldehyde and Derivatives. *J. Org. Chem.* **2010**, *75* (10), 3208−3213.

(4) Barszcz, B. Coordination Properties of Didentate N,O Heterocyclic Alcohols and Aldehydes towards Cu(II), Co(II), Zn(II) and Cd(II) Ions in the Solid State and Aqueous Solution. *Coord. Chem. Rev.* **2005**, *249*, 2259−2276.

(5) Casas, J. S.; Castiñeiras, A.; Rodríguez-Argüelles, M. C.; Sánchez, A.; Sordo, J.; Vázquez-López, A.; Vázquez-López, E. M. Diorganotin-(IV) Complexes of Imidazole-2-Carbaldehyde Thiosemicarbazone (H2ImTSC). The Crystal and Molecular Structures of the "free" Ligand and of [SnMe2(ImTSC)]. *J. Chem. Soc. Dalt. Trans.* **2000**, *14*, 2267−2272.

(6) Perl, N. R.; Leighton, J. L. Enantioselective Imidazole-Directed Allylation of Aldimines and Ketimines. *Org. Lett.* **2007**, *9*, 3699−3701.

(7) Efthymiou, C. G.; Raptopoulou, C. P.; Psycharis, V.; Tasiopoulos, A. J.; Escuer, A.; Perlepes, S. P.; Papatriantafyllopoulou, C. Copper(II)/di-2-Pyridyl Ketone Chemistry: A Triangular Cluster Displaying Antisymmetric Exchange versus an 1D Coordination Polymer. *Polyhedron* **2013**, *64*, 30−37.

(8) Efthymiou, C. G.; Papatriantafyllopoulou, C.; Aromi, G.; Teat, S. J.; Christou, G.; Perlepes, S. P. A NiII Cubane with a Ligand Derived from a Unique Metal Ion-Promoted, Crossed-Aldol Reaction of Acetone with Di-2-Pyridyl Ketone. *Polyhedron* **2011**, *30*, 3022−3025.

(9) Liu, J.-L.; Lin, W.-Q.; Chen, Y.-C.; Gómez-Coca, S.; Aravena, D.; Ruiz, E.; Leng, J.-D.; Tong, M.-L. Cu(II)-Gd(III) Cryogenic Magnetic Refrigerants and Cu8Dy9 Single-Molecule Magnet Generated by in Situ Reactions of Picolinaldehyde and Acetylpyridine: Experimental and Theoretical Study. *Chem. - Eur. J.* **2013**, *19*, 17567−17577.

(10) Abufager, P. N.; Robles, R.; Lorente, N. FeCoCp3Molecular Magnets as Spin Filters. *J. Phys. Chem. C* **2015**, *119*, 12119−12129.

(11) Moro, F.; Biagi, R.; Corradini, V.; Evangelisti, M.; Gambardella, A.; De Renzi, V.; del Pennino, U.; Coronado, E.; Forment-Aliaga, A.; Romero, F. M. Electronic and Magnetic Properties of Mn12 Molecular Magnets on Sulfonate and Carboxylic Acid Prefunctionalized Gold Surfaces. *J. Phys. Chem. C* **2012**, *116*, 14936−14942.

(12) Serrano, G.; Wiespointner-Baumgarthuber, S.; Tebi, S.; Klyatskaya, S.; Ruben, M.; Koch, R.; Müllegger, S. Bilayer of Terbium Double-Decker Single-Molecule Magnets. *J. Phys. Chem. C* **2016**, *120*, 13581−13586.

(13) Woodruff, D. N.; Winpenny, R. E. P.; Layfield, R. A. Lanthanide Single-Molecule Magnets. *Chem. Rev.* **2013**, *113*, 5110−5148.

(14) Cho, J. H.; Harrowfield, J.; Kim, J. Y.; Kim, Y.; Lee, Y. H.; Ohto, K.; Thuéry, P.; Won, M. S.; Woo, A. Some Post-Wernerian Coordination Chemistry. *Polyhedron* **2013**, *52*, 1190−1198.

(15) Cruz-Enriquez, A.; Baez-Castro, A.; Hopfl, H.; Parra-Hake, M.; Campos-Gaxiola, J. J. Tetrakis(u-Acetato-k2O:O′)-bis[(3-Pyridinecarboxaldehyde-kN′)]-dicopper(II) (Cu—Cu). *Acta Crystallogr., Sect. E: Struct. Rep. Online* **2012**, *68*, m1339−m1340.

(16) Li, Y.; Liu, Z.; Deng, H. Dichloridobis(pyridine-3-Carbaldehyde-kN)zinc(II). *Acta Crystallogr., Sect. E: Struct. Rep. Online* **2007**, *63*, m3065.

(17) Müller, B.; Vahrenkamp, H. Zinc Complexes of Aldehydes and Ketones, Zinc Complexes of Chelating Aldehydes. *Eur. J. Inorg. Chem.* **1999**, *1999*, 137−144.

(18) Wang, W.; Spingler, B.; Alberto, R. Reactivity of 2-Pyridine-Aldehyde and 2-Acetyl-Pyridine Coordinated to [Re(CO)3]+ with Alcohols and Amines: Metal Mediated Schiff Base Formation and Dimerization. *Inorg. Chim. Acta* **2003**, *355*, 386−393.

(19) Cox, M.; Newman, P.; Stephens, F.; Vagg, R.; Williams, P. Chiral Metal Complexes 40*. The Sterically Mediated Hydrolysis of a Coordinated Imine. *Inorg. Chim. Acta* **1994**, *221*, 191−196.

DOI: 10.1021/acs.jpca.6b07898
J. Phys. Chem. A 2016, 120, 7778−7785

(20) Bravo-García, L.; Barandika, G.; Bazán, B.; Urtiaga, M. K.; Arriortua, M. I. Thermal Stability of Ionic Nets with CuII Ions Coordinated to Di-2-Pyridyl Ketone: Reversible Crystal-to-Crystal Phase Transformation. *Polyhedron* **2015**, *92*, 117−123.
(21) Thangavel, A.; Elder, I. A.; Sotiriou-Leventis, C.; Dawes, R.; Leventis, N. Breaking Aggregation and Driving the Keto-to-Gem-Diol Equilibrium of the N,N′-Dimethyl-2,6-Diaza-9,10-Anthraquinonediium Dication to the Keto Form by Intercalation in cucurbit[7]uril. *J. Org. Chem.* **2013**, *78*, 8297−8304.
(22) Yonekawa, M.; Furusho, Y.; Sei, Y.; Takata, T.; Endo, T. Synthesis and X-Ray Structural Analysis of an Acyclic Bifunctional Vicinal Triketone, Its Hydrate, and Its Ethanol-Adduct. *Tetrahedron* **2013**, *69*, 4076−4080.
(23) Liu, B. Crystal Structure of Trans-diacetatobis(2,6-pyridinediylbis(3-Pyridinyl)-Methanone)-κ2N,N′)-copper(II) Acetonitrile (1/2), C42H28CuF6N8O8. *Z. Kristallogr. - New Cryst. Struct.* **2013**, *228*, 389−390.
(24) Maass, G.; Ahrens, M. L.; Schuster, P.; Winkler, H. Kinetic Study of the Hydration Mechanism of Vitamin B6 and Related Compounds. *J. Am. Chem. Soc.* **1970**, *92*, 6134−6139.
(25) Helmreich, E. J. M.; Klein, H. W. The Role of Pyridoxal Phosphate in the Catalysis of Glycogen Phosphorylases. *Angew. Chem., Int. Ed. Engl.* **1980**, *19*, 441−455.
(26) O'Leary, M.; Payne, J. 13C NMR Spectroscopy of Labeled Pyridoxal 5′-Phosphate. *J. Biol. Chem.* **1976**, *251*, 2248−2254.
(27) Hanes, J. W.; Keresztes, I.; Begley, T. P. 13C NMR Snapshots of the Complex Reaction Coordinate of Pyridoxal Phosphate Synthase. *Nat. Chem. Biol.* **2008**, *4*, 425−430.
(28) Chan-Huot, M.; Niether, C.; Sharif, S.; Tolstoy, P. M.; Toney, M. D.; Limbach, H. H. NMR Studies of the Protonation States of Pyridoxal-5′-Phosphate in Water. *J. Mol. Struct.* **2010**, *976*, 282−289.
(29) Fung, B. M.; Khitrin, A. K.; Ermolaev, K. An Improved Broadband Decoupling Sequence for Liquid Crystals and Solids. *J. Magn. Reson.* **2000**, *142*, 97−101.
(30) Sheldrick, G. M. Phase Annealing in SHELX-90: Direct Methods for Larger Structures. *Acta Crystallogr., Sect. A: Found. Crystallogr.* **1990**, *46*, 467−473.
(31) Sheldrick, G. M. A Short History of SHELX. *Acta Crystallogr., Sect. A: Found. Crystallogr.* **2008**, *64*, 112−122.
(32) Athimoolam, S.; Natarajan, S. Nicotinium Trifluoroacetate. *Acta Crystallogr., Sect. E: Struct. Rep. Online* **2007**, *63*, o2656−o2656.
(33) Baias, M.; Widdifield, C. M.; Dumez, J.-N.; Thompson, H. P. G.; Cooper, T. G.; Salager, E.; Bassil, S.; Stein, R. S.; Lesage, A.; Day, G. M.; et al. Powder Crystallography of Pharmaceutical Materials by Combined Crystal Structure Prediction and Solid-State 1H NMR Spectroscopy. *Phys. Chem. Chem. Phys.* **2013**, *15*, 8069−8080.
(34) Mantero, D. G.; Altaf, M.; Neels, A.; Stoeckli-Evans, H. Pyridin-4-Ylmethanediol: The Hydrated Form of Isonicotinaldehyde. *Acta Crystallogr., Sect. E: Struct. Rep. Online* **2006**, *62*, o5204−o5206.
(35) Majerz, I.; Sawka-Dobrowolska, W.; Sobczyk, L. Hydrogen Bonds in 4-Dihydroxymethylpyridinium 2,6-Dichloro-4-Nitrophenolate. *J. Mol. Struct.* **1997**, *416*, 113−120.
(36) Bock, H.; Van, T. T. H.; Schödel, H.; Dienelt, R. Structural Changes of Di(2-Pyridyl) Ketone on Single and Twofold Protonation. *Eur. J. Org. Chem.* **1998**, *1998*, 585−592.
(37) Sue-Lein, W.; Richardson, J. W.; Briggs, S. J.; Jacobson, R. A.; Jensen, W. P. Stabilization of a Hydrated Ketone by Metal Complexation. The Crystal and Molecular Structures of Bis-2,2′,N,N′-Bipyridyl Ketone-Hydrate Nickel(II) Sulfate, Copper(II) Chloride and Copper(II) Nitrate. *Inorg. Chim. Acta* **1986**, *111*, 67−72.
(38) Yang, G.; Tong, M. L.; Chen, X. M.; Ng, S. W. Bis(di-2-Pyridylmethanediol-N,O,N′)- copper(II) Diperchlorate. *Acta Crystallogr., Sect. C: Cryst. Struct. Commun.* **1998**, *54*, 732−734.
(39) Gansow, O. A.; Holm, R. H. Aqueous Solution Equilibria of Pyridoxamine, Pyridoxal, 3-Hydroxypyridine-4-Aldehyde, and 3-Hydroxypyridine-2-Aldehyde as Studied by Proton Resonance. *Tetrahedron* **1968**, *24*, 4477−4487.
(40) Sudhakar Rao, S. P.; Damodara Poojary, M.; Manohar, H. Crystal and Molecular Structure of Pyridoxal. *Curr. Sci.* **1982**, *51*, 410−411.
(41) Fujiwara, T.; Izumi, Y.; Tomita, K. The Crystal and Molecular Structures of Vitamin B6 Derivatives. *Acta Crystallogr. Sect. A Cryst. Phys., Diffr., Theor. Crystallogr.* **1972**, *28*, S49.
(42) Fujiwara, T. The Crystal and Molecular Structure of Vitamin B6 Derivatives. I. Pyridoxal Phosphate Hydrate and Pyridoxal Phosphate Methyl Hemiacetal. *Bull. Chem. Soc. Jpn.* **1973**, *46*, 863−871.

DOI: 10.1021/acs.jpca.6b07898
J. Phys. Chem. A 2016, 120, 7778−7785